Long-term variability in overwintering copepod populations in the Lofoten Basin: The role of the North Atlantic oscillation and trophic effects

Nicolas Weidberg [ORCID],* Sünnje L. Basedow
Arctic and Marine System Ecology, Faculty of Biosciences, Fisheries and Economics, UiT - The Arctic University of Norway, Tromsø, Norway

Abstract

Critical gaps in knowledge hinder our ability to infer spatiotemporal dynamics in pelagic ecosystems. In particular, environmental changes affecting key copepod species while overwintering in deep waters are still not well understood. Here, we analyzed an 11 yr time series (2000–2010) of winter (January/February) samplings in the Lofoten Basin to characterize the spatial distribution of *Calanus finmarchicus* overwintering abundances and to infer their long-term temporal trends. The spatial structure of populations at depths between 700 and 900 m corresponded to mesoscale aggregations consistent with eddies in the region. Over time, increased abundances of copepods and of one of its main predators, the herring (*Clupea harengus*), matched a negative trend in the 7 yr lagged winter NAO index. However, this progressive climatic shift did not affect surface conditions in the region or southward but corresponded to an increase in salinity and a deepening of the vertical extension of the Atlantic Water layer. We hypothesized that this change in salinity structure across the water column increased the density contrast between copepods and ambient water masses and facilitates the ascent rates during seasonal vertical migration. We suggest a step-wise mechanism from NAO large-scale forcing to copepod and herring populations mediated by hydrographical changes in intermediate water masses to explain the observed trends in abundances. Thus, large-scale, lagged climatic patterns affecting overwintering copepods might scale up to successive trophic levels in the pelagic ecosystem.

Major spatiotemporal shifts in pelagic ecosystems have occurred recurrently over vast oceanic and coastal regions in the past and are ocurring increasingly today (IPCC Fifth Report 2014). For instance, increased westward winds over the western Indian Ocean and the associated deepening of the thermocline and reduction of primary production have been observed repeatedly (Currie et al. 2013; Lan et al. 2013). Along the Pacific coast of South America, the recurrent weakening of westward trade winds promotes the cessation of upwelling and productivity during El Niño (Barber et al. 1996). In the Eastern North Atlantic and Arctic, the freshening and cooling of the Atlantic inflow since the late 1960s to the early 1990s, and the subsequent reversal, affected sea surface temperature (SST) and primary production (Jakobsson 1969; Curry et al. 2003; Tiselius et al. 2016). In all these cases, changes in the planktonic community scaled up through the trophic web eventually affecting key fisheries (yellowfin tuna, peruvian anchovy, herring, and cod, respectively) whose collapses caused severe economic and social problems in modern societies (Changnon 1999; Hamilton et al. 2004). These trophic cascading effects and their impacts, usually exacerbated and sometimes triggered by overfishing, have been widely studied and described (e.g., Beaugrand and Kirby 2010; Pershing et al. 2015*a,b*), but the mechanisms and species-specific underlying processes behind the long-term changes remain largely unknown. This is partly due to the lack of knowledge of the biology of individual species (Sale et al. 2005; Urban et al. 2016) and partly due to the lack of long-term and large-scale data on the distribution of prey and predator species (Tittensor et al. 2003). In the last decades, it has become crucial to fill these knowledge gaps to better understand how populations can cope with environmental changes due to natural and anthropogenic climatic fluctuations (Ullah et al. 2018) and to be able to predict how the marine ecosystem will respond to such changes.

Few keystone planktonic species can serve as model organisms to analyze long-term environmental forcing on their populations, because this requires a good knowledge of the species' life cycle and a good historical record of abundances over large areas. One well-studied species is the copepod *Calanus finmarchicus* (Gunnerus, 1770), which frequently contributes > 50% to total mesozooplankton biomass in the North Atlantic and subarctic Nordic Seas (Planque and Batten 2000;

Carstensen et al. 2012). It is the main prey item for a wide range of predators, including predatory copepods, medusae, krill, chaetognaths, herring, mackerel, blue whiting, mesopelagic fish, and right whales (Baumgartner et al. 2003; Falk-Petersen et al. 2009; Bachiller et al. 2016). In recent years, humans also started exploiting the species in the Norwegian Sea, where copepods are harvested to obtain oil-derived products for dietary use (Vang 2015). At its main population centers in the Nordic Seas *C. finmarchicus* has a 1-yr life cycle that consists of two contrasting phases: active feeding and reproduction in surface waters during few months in spring and summer and a longer dormancy phase, called diapause, at great depths in autumn and winter (Gaardsted et al. 2011; Melle et al. 2014).

A major long-term forcing that affects *C. finmarchicus* and its habitat in the North Atlantic and Nordic Seas is described by the North Atlantic Oscillation (NAO) index, defined as the normalized difference in sea surface pressure between the Icelandic low pressure and the Azores Anticyclone (Fromentin and Planque 1996; Beaugrand 2003; Kimmel and Hameed 2008). High values of the NAO index are indicative of an increased flow of the Atlantic Current to the northeast and into the Norwegian Sea, whereas low NAO indices indicate a reduced Atlantic Water (AW) inflow into the Nordic Seas (Hurrell 1995; Visbeck et al. 2001). In the long term, prolonged atmospheric NAO forcing is transmitted across the whole North Atlantic and into the Nordic Seas with characteristic time lags due to the effective pathway through different water masses along horizontal and vertical axes (Yashayaev 2007; Sarafanov 2009). In the Northwestern Atlantic, positive trends in the abundances of *C. finmarchicus* were observed to coincide with positive NAO forcing and higher SSTs with a lag of 1–2 yr (Conversi et al. 2001). Contrasting patterns have been observed in the Northeastern Atlantic between 45°N and 65°N, where surface *C. finmarchicus* abundances decreased with increasing SST as the NAO index increased from 1960 to 1999 (Fromentin and Planque 1996; Beaugrand et al. 2002). However, the importance of the NAO in explaining *Calanus* sp. abundances was susbtantially reduced when temporal autocorrelation and detrending analyses were applied (Kimmel and Hameed 2008). Therefore, it is of particular importance to account for common trends in time series prior to establish causal relationships when exploring potential oceanographic mechanisms behind the dynamics of planktonic populations (Kimmel and Hameed 2008).

The overwintering habitat in the northern Norwegian Sea was identified as a potential source in explaining increased summer abundances in several seas downstream (Heath et al. 2000; Aarflot et al. 2017). Both in the Fram Strait and in the Barents Sea, *C. finmarchicus* abundance increased over the last decades, from 2001 to 2009 in the Fram Strait and from 1995 to 2016 in the Barents Sea (Carstensen et al. 2012; Aarflot et al. 2017). Increasing salinity in the Atlantic Water was observed during the same time, and significant statistical relationships between salinity and *C. finmarchicus* have been found (Daase

et al. 2007; Carstensen et al. 2012). However, the species-specific biological processes underlying such an association are not clear. Processes related to overwintering dynamics might provide cues for a mechanistical explanation of statistical relationships. Recent research based on the expression of a number of clock genes in *C. finmarchicus* during the seasonal cycle indicates that diapause is initiated individually, while it is terminated in a synchronized way at the scale of the whole population at a fixed time (Häfker et al. 2018). Termination seems to be triggered by a circannual clock that is entrained in the copepods while they occupy the surface layer during spring (Häfker et al. 2018). Initiation seems to be triggered by a combination of day length, temperature, food, and the lipid reserves that the copepod has accumulated (Hirche 1996; Baumgartner and Tarrant 2017; Häfker et al. 2018; Schmid et al. 2018). The duration of diapause for individual copepods within a population will thus vary, and this affects the remaining lipid reserves during the emergence period in spring (Tittensor et al. 2003; Johnson et al. 2007).

Lipid contents also determine the buoyancy of copepods, and the instability in biochemical composition of the lipids might facilitate vertical migrations (Campbell and Dower 2003). After lipid accumulation in surface waters during spring and summer, buoyant lipids prevent sinking (Yayanos et al. 1978), but active downward swimming against upward buoyancy forces is compensated with depth as lipid density increases with pressure and in turn copepod density increases (Visser and Jonasdottir 1999). Neutral buoyancy might be reached at overwintering depth, thus enabling the copepods to remain at a relatively fixed depth without actively swimming. In spring, the ascent might be largely passive, aided by increased buoyancy as lipid density decreases (Ingvarsdóttir et al. 1999; Visser and Jonasdottir 1999). During diapause, only the most dense lipids are consumed thus allowing a largely passive ascent in spring driven by lighter lipid components (Pond 2012). These complex processes of lipid accumulation, seasonal migrations, and overwintering in combination with environmental factors alter individual state and affect population dynamics. Large-scale climatic forcing drives major hydrographic changes in the AW layer, which are eventually transmitted to deeper water masses that constitute the habitat of diapausing *C. finmarchicus* (Curry et al. 2003). However, as there are few long-term wintertime samplings (Tittensor et al. 2003), our ability to study overwintering populations in relation to large spatiotemporal climatic shifts is limited.

In this study, we aim (1) to characterize the spatiotemporal structure of overwintering *C. finmarchicus* in the northern Norwegian Sea, (2) to test which climatic and environmental factors experienced by copepods at surface and depth contribute to the overwintering population size, and (3) to test if temporal variations in the *C. finmarchicus* overwintering stock scale up in the trophic web affecting the Norwegian spring spawning herring. We base our analyses on an extensive time series of overwintering abundances of *C. finmarchicus* in the northern Norwegian Sea between 2000 and 2010. These data

are paired with the large-scale NAO index, with satellite data on temperature and chlorophyll *a* (Chl *a*) to characterize the surface habitat, with in situ values of salinity to characterize the water column habitat, and with estimates of the spawning stock of the Norwegian spring spawning herring to investigate trophic effects.

Material and methods

Study area

Our study area in the northern Norwegian Sea lies in the Lofoten Basin off the coast of northern Norway (Fig. 1). The saline, warm Norwegian Atlantic Current flows over the basin as part of the Atlantic meridional overturning circulation (Fig. 1), thus the area is affected by poleward advection toward the Barents Sea and Svalbard. However, within the deeper Arctic water mass (> ca. 800 m deep), southwestward currents have been detected, which in combination with persistent anticyclonic eddies could enhance retention in the Lofoten Basin (Fig. 1; Orvik 2004, Soiland and Rossby 2013). The phytoplankton spring bloom normally starts by the end of March in the southeastern domain of the Lofoten Basin closer to the shelf and propagates to the northwest thus affecting the entire basin by mid April. This peak in phytoplankton biomass is closely followed by the life cycle of the dominant zooplankter in the region, *C. finmarchicus*. The overwintering generation (copepodite V and adults) ascend to the surface, feed on enhanced primary production, and spawn (Slagstad and Tande 1996). The next generation grows to copepodite stages IV–V in

surface waters and then descends to depths below the AW layer within the Norwegian Sea Deep Water (600–1000 m) to again overwinter in diapause (Halvorsen et al. 2003). In turn, the Norwegian spring spawning herring (*Clupea harengus*), one of the main copepod predators in the region, follows the spatiotemporal dynamics of *C. finmarchicus*. Although herring migration patterns are variable and have changed after the collapse of the fishery in the 1960s, in the last years, nursery areas have been located in the Barents Sea from where young adults around 5 yr old migrate to southern Norway to spawn off Møre at the beginning of spring and then move to the northeast toward the Lofoten Basin as the bloom progresses (Huse et al. 2012; Huse 2016).

Field sampling

Data on hydrography and zooplankton distribution were collected during 11 research cruises in January/February 2000 to 2010 on board R/V "*Jan Mayen*" (now called R/V "*Helmer Hanssen*"), as part of several research projects. A total of 604 stations in the Lofoten Basin and beyond (68°N–73.5°N, 4.5°E–19.9°E; Fig. 1) were sampled in search of overwintering *C. finmarchicus* stocks. Station depths ranged from 120 to 3250 m. To obtain vertical profiles of temperature, salinity, and density a conductivity-temperature-depth sensor (CTD; SBE 911plus, Seabird Electronics) was deployed at each station. Data on the vertical distribution of zooplankton were collected by a MultiNet Midi (equipped with five nets of 180 μm mesh size, 0.25 m^2 mouth opening, Hydrobios) and by a laser optical plankton counter (LOPC; ODIM-Brooke
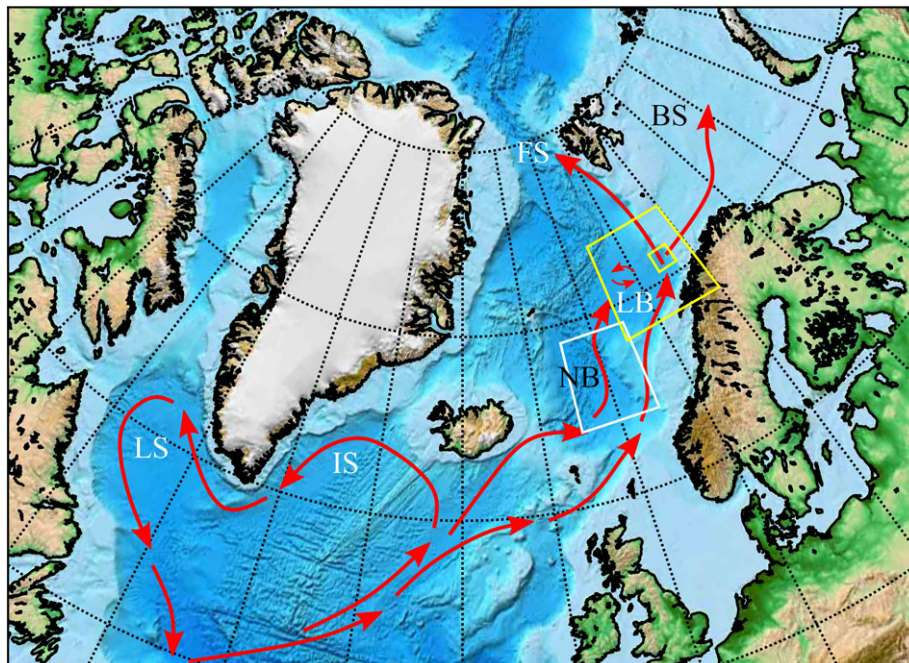
Fig. 1. North Atlantic and Arctic circulation patterns and study area. The large and small yellow rectangles show the whole study area and the focus area, respectively, whereas the white rectangle represents the Southern Source. Advective pathways are represented with red arrows. The main geographical areas are specified: from west to east, the Labrador Sea (LS), the Irminger Sea (IS), the Norwegian Basin (NB), the Lofoten Basin (LB), the Fram Strait (FS), and the Barents Sea (BS).

Table 1. Summary of the winter cruises analyzed in this study. Detailed description of the sampling methodologies used can be found in the references.

Years	Dates	Instrument	Depth range	Reference
2000–2002	02 January 2000–21 February 2000, 10 January 2001–25 January 2001, 16 January 2002–27 January 2002	Multinet type Midi	Onshelf: 0–100–200–300–500–bottom; Offshelf: 0–200–500–700–1200–1800	Halvorsen et al. (2003)
2003–2004	19 January 2003–30 January 2003, 16 February 2004–29 February 2004	Multinet type Midi	Onshelf: 0–100–200–300–500–bottom; Offshelf: 0–200–2°C, isotherm–0°C, isotherm–1200–1800	Edvardsen et al. (2006)
2005–2006	8 January 2005–21 January 2005, 24 January 2006–4 February 2006	Multinet type Midi	Onshelf: 0–200–300–400–500–bottom; Offshelf: 0–600–900–1200–1500–1800	Gaardsted et al. (2010b)
2007–2010	16 January 2007–28 January 2007, 18 January 2008–28 January 2008, 24 January 2009–30 January 2009, 11 January 2010–31 January 2010	LOPC	Consecutive 25 m intervals from 12.5 to 1837.5 m	Gaardsted et al. (2010b)

Ocean Rolls Royce Canada; Herman et al. 2004). From 2000 to 2006, the MultiNet was used exclusively, from 2007 onward MultiNet measurements were combined with and gradually replaced by LOPC measurements (Table 1). The LOPC had been calibrated against the Multinet and provided a good match (Pearson's correlation coefficients > 0.65) when estimating *C. finmarchicus* winter abundances (Gaardsted et al. 2010a). The area sampled was not constant over the years, but a common focus area (70.5°N–71.6°N, 13.7°E–17°E) was sampled during 8 yr (2003–2008 and 2010; Fig. 1).

Spatial variability in overwintering copepods

To evaluate the spatial distribution of overwintering *C. finmarchicus* populations, integrated abundances (individuals m^{-2}) over the entire water column were calculated for each station. Integrated abundances were then interpolated over the entire area sampled each year using the matplotlib function meshgrid in python (Hunter 2007). The visual inspection of these annual distributions reveals potential hotspots of overwintering copepods in the region. To estimate the patch size of copepod aggregations, Moran's *I* index of spatial autocorrelation was calculated at different distances, based on which spatial correlograms were constructed. Linear and exponential functions were fitted to the correlograms. The patch size is then estimated as the distance range at which Moran's *I* first decreases below zero, i.e., the distance at which copepod abundances are no longer correlated to each other (Zhang et al. 2006). Patch size analyses were performed for each year separately and for a data set with all stations in all years pooled. As patch size may be influenced by the total area sampled, each of the analyses was performed only for the focus area that was sampled during all years.

Weighted mean depths (WMDs) of copepods were computed as:

$$WMD = (\Sigma N_{sd} z_d)/(\Sigma N_s) \tag{1}$$

where N_s is the abundance (individual m^{-3}) at station s, z_d is the mean depth of sampling interval d, and N_{sd} is copepod abundance at depth interval d at station s.

Surface environment

To characterize the surface environment experienced by the copepods in the spring before overwintering, satellite-derived time series of SST and Chl *a* were retrieved from the Advanced Very High-Resolution Radiometer Pathfinder and from the SeaWiFS Orbview 2, respectively (https://coastwatch.pfeg.noaa.gov/erddap/griddap/erdPH2sstamday.html and https://coastwatch.pfeg.noaa.gov/erddap/griddap/erdSWchlamday.html). The monthly composite products provide a spatial resolution of 0.0417° for SST and 0.1° for Chl *a*. Satellite surface data sets were obtained from January 1999 to December 2010 and from two different areas, which were chosen based on known advection patterns of the copepods: the so-called Southern Source (64°N–69°N, 5°W–5°E) and the Lofoten Basin (68°N–73.5°N, 4.5°E–19.9°E; Fig. 1. From the Southern Source area (southern Norwegian Sea), copepods that inhabit the surface layer in spring are advected northeastward toward the Lofoten Basin with prevailing currents (Sætre 2007) and might descend to overwintering depths in our study area. In addition, copepods overwintering along the slope in the Southern Source area might be transported with the deep circulation toward the Lofoten Basin (Soiland and Huse 2012). However, retention in the Lofoten Basin might be higher than previously thought (Soiland and Rossby 2013), therefore copepods that develop in the surface layer within the Lofoten Basin might also contribute to overwintering stocks observed there. In both areas, temporal trends in surface environmental variability were analyzed by fitting Generalized Additive Models (GAMs) to monthly composite SST and Chl *a* data that were

averaged over each area (Southern Source and Lofoten Basin). These statistical analyses allow for the quantification and removal of seasonality, thus enabling the calculation of long-term trends in time series with a strong seasonal cycle. Furthermore, the GAM analyses are robust against the presence of gaps and zeros in the data set (Wood 2006). The GAMs were set up as following:

$$y = \alpha + s(Y) + s(T) + \varepsilon \tag{2}$$

where y stands for the dependent variable (SST or Chl a, respectively), $s(Y)$ and $s(T)$ are smoothed yearly and seasonal trends, respectively, α is a constant, and ε is the error term. The GAMs were also formulated with an autoregressive model to analyze the residuals.

Water column environment

Hydrographical data were analyzed to evaluate the environmental conditions experienced by the copepods during their seasonal vertical migrations. CTD data were screened for values out of range, and the remaining data were averaged over depth ranges sampled by the MultiNet (Table 1), or over 20 m bins if the LOPC was used. In 2003, the conductivity sensor failed and salinity data could not be obtained (Edvardsen et al. 2006). The depth layer over which the AW (salinity > 35; Mork and Skagseth 2010) stretched was identified by regressing salinity against depth using a local weighted smoothing (LOESS) fit (Fig. 2). Once these depths were determined for each year, average salinities were calculated within the AW layer.

Climatic effects

Climatic effects were assessed based on monthly indices of the NAO index, which were retrieved for the years 1985 to 2010 from https://www.ncdc.noaa.gov/teleconnections/nao/. To analyze seasonality and long-term trends, a GAM was set up as in Eq. 2 but with y being the NAO index. For this analysis, only the years 1999 to 2010 were considered. To evaluate the influence of large-scale climatic forcing on the water column environment, from the monthly NAO index, five-winter (September to January) running averages were computed. The use of moving arithmetic averages of NAO monthly indices over the previous five winters is a smoothing procedure commonly applied to the index prior to comparisons over large spatial scales (Lozier and Stewart 2008; Sarafanov 2009). Average salinity within the AW layer for each year (2000 to 2011) was then linearly regressed against the five-winter NAO. These linear regressions were performed using different time lags, from 0 to 15 yr, to test for time lags of climatic effects. The best fit of the average salinity within the AW layer against five-winter NAO index was obtained at a lag of 7 yr (Fig. 3), consequently the wintertime NAO index at a lag of 7 yr was used for correlation analyses with biological data sets.
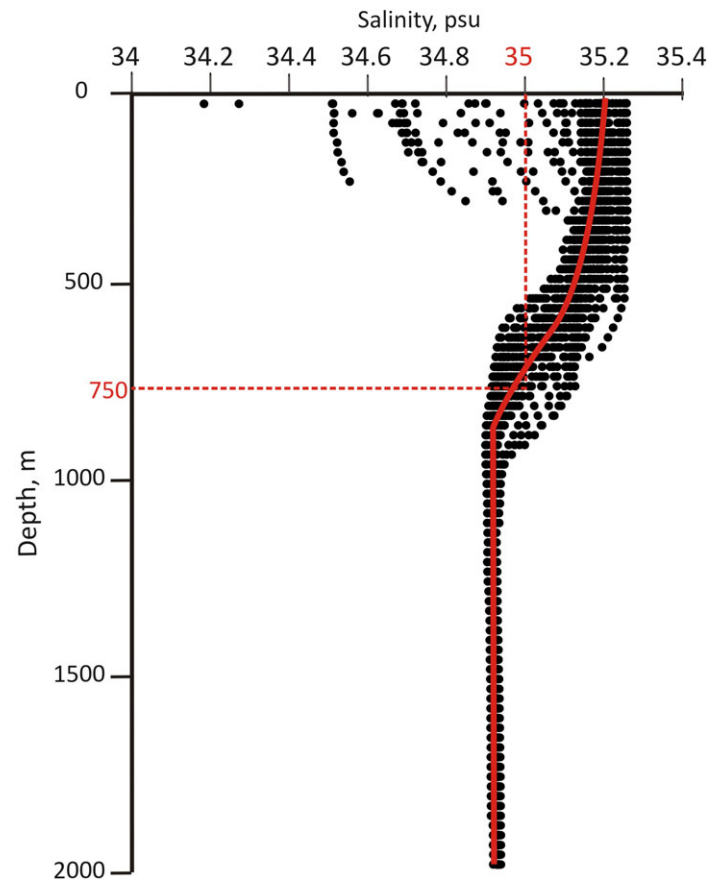

Fig. 2. Salinity vertical profiles for 2009. The red line represents the LOESS fit. Red dashed lines and numbers show the depth (750 m) at which a value of 35 psu is attained according to the fit.

Long-term trends

Temporal trends in mean overwintering abundance were regressed against mean SST and Chl a in the spring/summer (March–September) before each winter cruise to infer whether surface conditions influenced overwintering populations. These relationships were investigated for the Southern Source and the Lofoten Basin separately.

To investigate long-term trends and interactions among climatic effects, environment, and biota, each of the following variables were regressed against time and against each other: the NAO index at a lag of 7 yr, mean salinity within the AW layer, thickness of the AW layer, copepod abundance, WMD of copepods, and spawning stock biomass (SSB) of the Norwegian spring spawning herring. Linear regressions between variables exhibiting a significant temporal common trend were not carried out to avoid an undesired increase in type II error rates (acceptance of the null hypothesis when it should be rejected). Instead, Kendall's τ indices of rank correlations were calculated, as these are not affected by linear dependency (Buonaccorsi et al. 2001).

Annual time series of the SSB of the Norwegian spring spawning herring (*C. harengus*) were retrieved from the International Council for the Exploration of the Sea (ICES)
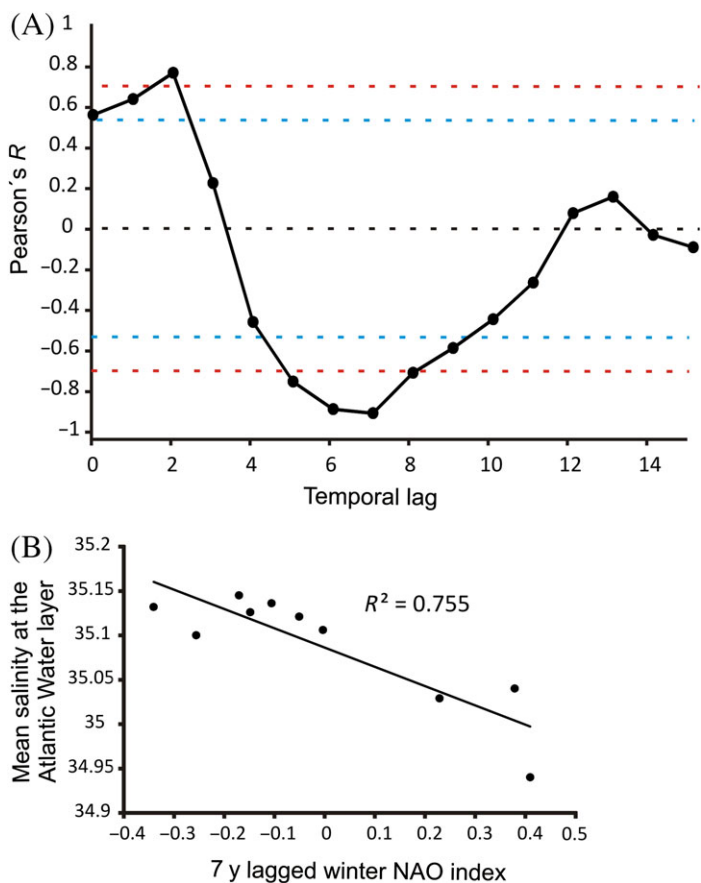
Fig. 3. (**A**) Pearson's R for regressions between the width of the Atlantic layer (35 psu) and the five winter running average of the NAO index at different temporal lags. Dashed lines mark a Pearson's R value of 0 (black line), and significance levels at $p = 0.05$ (blue line) and $p = 0.0033$ (Bonferroni correction, red line). (**B**) Best linear regression between mean salinity and winter NAO index with a lag of 7 yr.

database for the years 1999 to 2010 (http://standardgraphs. ices.dk/ViewCharts.aspx?key=9244).

Results

Spatiotemporal variability in overwintering copepods

The horizontal distributions of overwintering copepods displayed variable patterns between the years (Fig. 4). In 2000, high abundances of up to 150,000 individuals m^{-2} were observed along the shelf break (10°E–15°E, 70°N–72°N). In contrast, in 2001 and 2002, similar high densities were only observed at some stations north of 69°N. In 2003 and 2004, overall abundances were relatively low, whereas 2005 onward often abundances of > 100,000 individuals m^{-2} were recorded along the shelf break. Also, in the focus area, lower abundances from 2003 and 2004 were followed by years of higher densities. However, in 2010, abundances decreased again. Pooling all years, a patch size of 31 km was estimated based on Moran's I values (Fig. 5). When spatial correlograms were considered for each year separately, significant fits were only
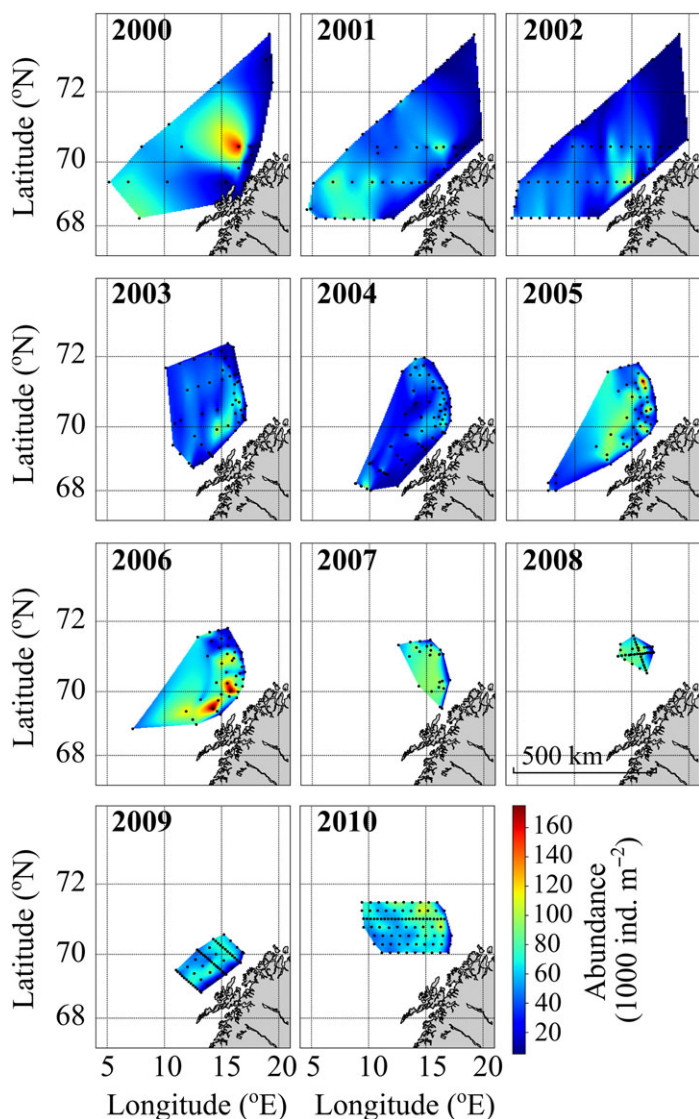

Fig. 4. Integrated abundance of overwintering *Calanus* sp. in the Lofoten Basin, from 2000 to 2010.

obtained for 2008 (Table 2). Significant patch sizes then ranged from 41 to 133 km (Table 2).

In all years, overwintering copepods were observed at depths below the AW layer. The water column was dominated by AW in the upper 450 to 750 m, approximately. Both the width of the AW layer and the mean salinity within the layer increased significantly over the years (Fig. 6). Salinity maxima of 35.2–35.3 were reached between 300 and 500 m depth (Fig. 2). The thickness of the AW layer and the copepods´ WMD significantly increased with time (Fig. 6). Both time series were positively and significantly correlated according to Kendall's τ estimates (Fig. 6).

Long-term trends—surface environment

Time series of SST and Chl a at the Southern Source and within the Lofoten Basin did not show any consistent long-
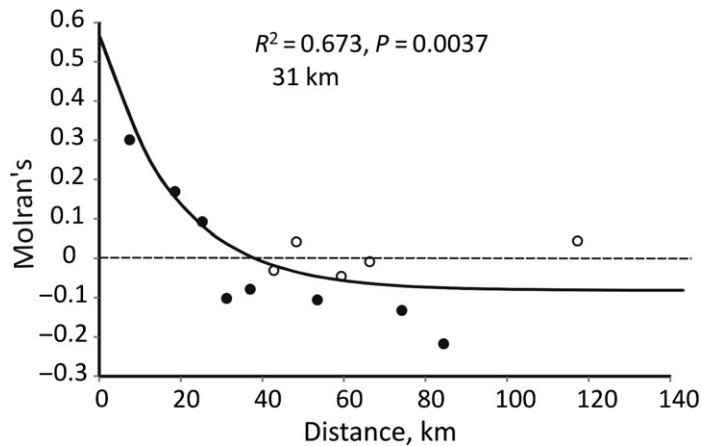
Fig. 5. Spatial correlograms for the focus area based on copepod abundances in individuals m^{-2}. Data from all available years were pooled together. An exponential fit is shown with dark lines. Dashed lines mark null Moran's *I*, the value used to calculate patch size. This patch size in kilometer together with variance explained and statistical significance are also shown. Dark and white dots point to significant and nonsignificant individual Moran's *I* values, respectively, at an α value of 0.05.

Table 2. Spatial correlogram parameters for each cruise considering the fixed focus area region (see Material and Methods for exact locations). Figures in bold letters show parameters for significant linear fits to Moran's *I* correlogram values.

Year	Patch size	R^2	*p*	*N*
2003	44.54	0.5237	0.104	14
2004	73.03	0.0655	0.5767	17
2005	73.66	0.1779	0.4049	13
2006	44.58	0.3557	0.2115	15
2007	20.56	0.2586	0.3029	14
2008	**41.62**	**0.6573**	**0.0025**	**69**
2010	133	0.0153	0.7706	25

term trend in time (Fig. 7). As expected, the seasonal component of the GAMs revealed a strong cycle with higher temperatures and Chl *a* in summer and spring, respectively. In contrast, the annual long-term component did not exhibit any marked trend. However, Chl *a* in the Southern Source decreased slightly from 1999 to 2010, (Fig. 7A). Conversely, no seasonal pattern in the NAO index was observed, but the index decreased significantly over the years, especially marked between 2008 and 2010 (Fig. 7E).

Long-term trends—water column

Long-term changes were detected in the hydroclimatic forcing and in the AW layer: the 7-yr lagged winter NAO index significantly decreased with time (Fig. 8A), whereas mean salinity of the AW layer increased with time (Fig. 8B). Also, mean overwintering copepod abundances per year significantly increased with time from 2000 to 2010 (Fig. 8C). These trends indicate a sustained increase of 4000 individuals m^{-2} yr^{-1}, approximately.
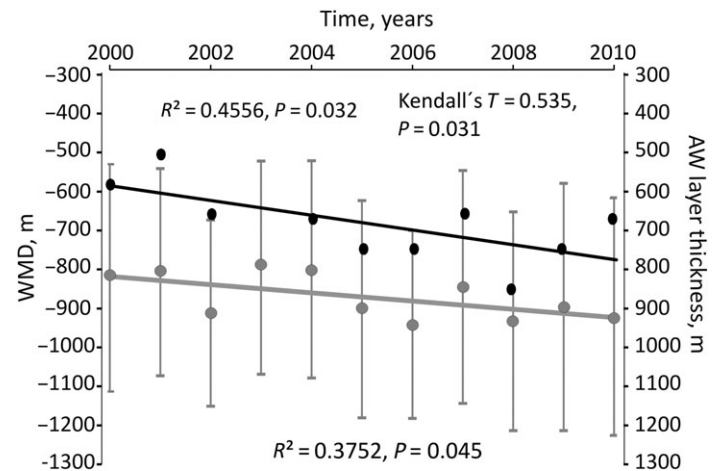

Fig. 6. Time series of the AW layer thickness and copepod WMD (black and gray lines, respectively) with their respective variance explained and statistical significance. For MLD time series, bars represent standard deviations. Results of the correlation between the two time series (Kendall τ analyses) are also shown.

To our surprise, the observed increase was not explained by surface environmental variables from the previous spring. When averaged between March and September for both the Southern Source and the Lofoten Basin, SST and Chl *a* did not correlate with winter copepod abundances, with R^2 values between 0.03 and 0.21 and *p* values between 0.61 and 0.15. However, the SSB of the Norwegian spring spawning herring significantly increased in the same period at a rate of 350,000 t yr^{-1} (Fig. 7D). When these variables were correlated with each other, Kendall's τ analyses were applied as all of the variables exhibited significant temporal trends. High levels of correspondence were revealed by the statistical analyses (Table 3). Only the pair-wise comparison between the width of the AW layer and mean overwintering copepod abundance was nonsignificant, albeit only slightly so (Table 3). All other variables were significantly related, i.e., increasing abundances of copepods and higher herring biomass were correlated with saltier, deeper AW layers, which in turn were negatively associated with the 7-yr lagged wintertime NAO (Table 3).

Discussion

In this study of the overwintering *Calanus sp.* population in the Lofoten Basin from 2001 to 2010, patch sizes between 41 and 133 km were observed, which corresponds to the size of mesoscale eddies in the region (Pedersen et al. 2005). Overwintering abundance increased during the time period, and correlated with an increase in AW salinity that was driven by a lagged effect of the NAO. Overwintering abundance did not correlate with either temperature or food (Chl *a*) in surface waters the previous spring. Thus, a shift in the surface environment experienced by actively feeding and reproductive stages did not explain the observed temporal trends. This
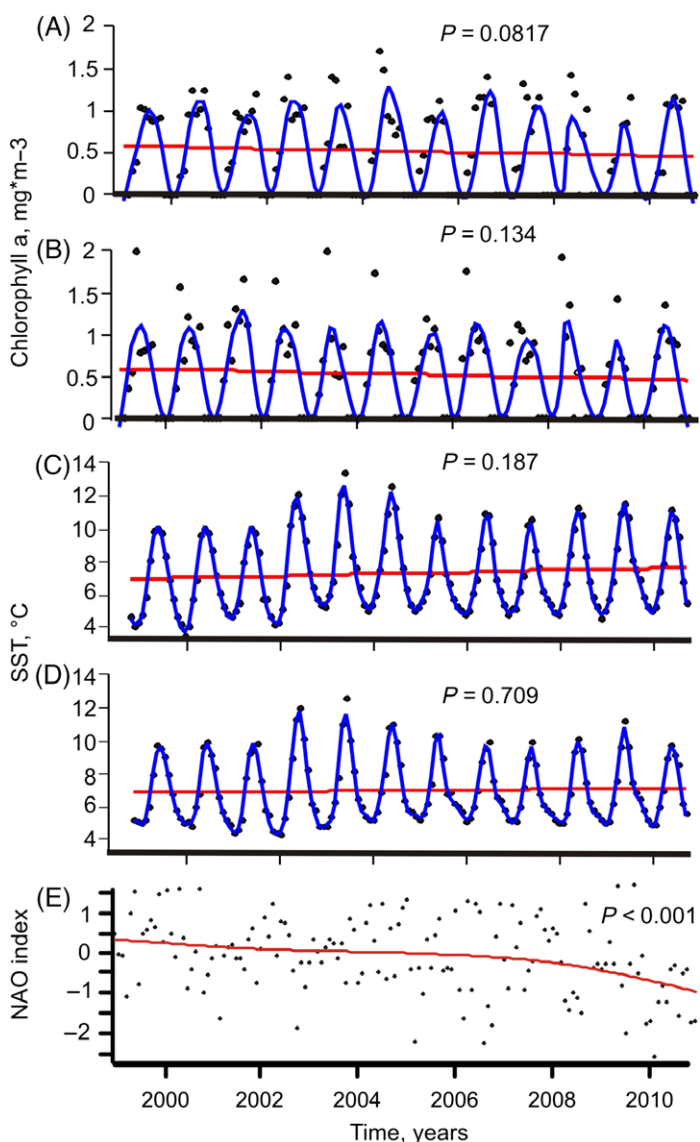
Fig. 7. Time series of satellite-derived SST and Chl *a* (for the Southern Source [**A**, **C**] and the Lofoten Basin [**B**, **D**]) and of the NAO monthly index (**E**). The red and blue lines represent the long-term and seasonal components of the general additive models, respectively. Statistical significance is shown for the long-term trend.

suggests that spatiotemporal patterns of overwintering *Calanus* sp. abundance in the Lofoten Basin are driven by climatic and physical factors transmitted through the AW layer, and that the surface environment experienced by the copepods during spring and summer is of lesser importance.

Spatial patterns in abundance

Observed significant patch sizes (between 41 and 133 km) correspond to oceanographic features on the mesoscale (tens to hundreds of kilometers; Fig. 5; Table 2). Mesoscale eddies are produced by instabilities between the saltier Norwegian Atlantic Current and the Norwegian Coastal Current as both
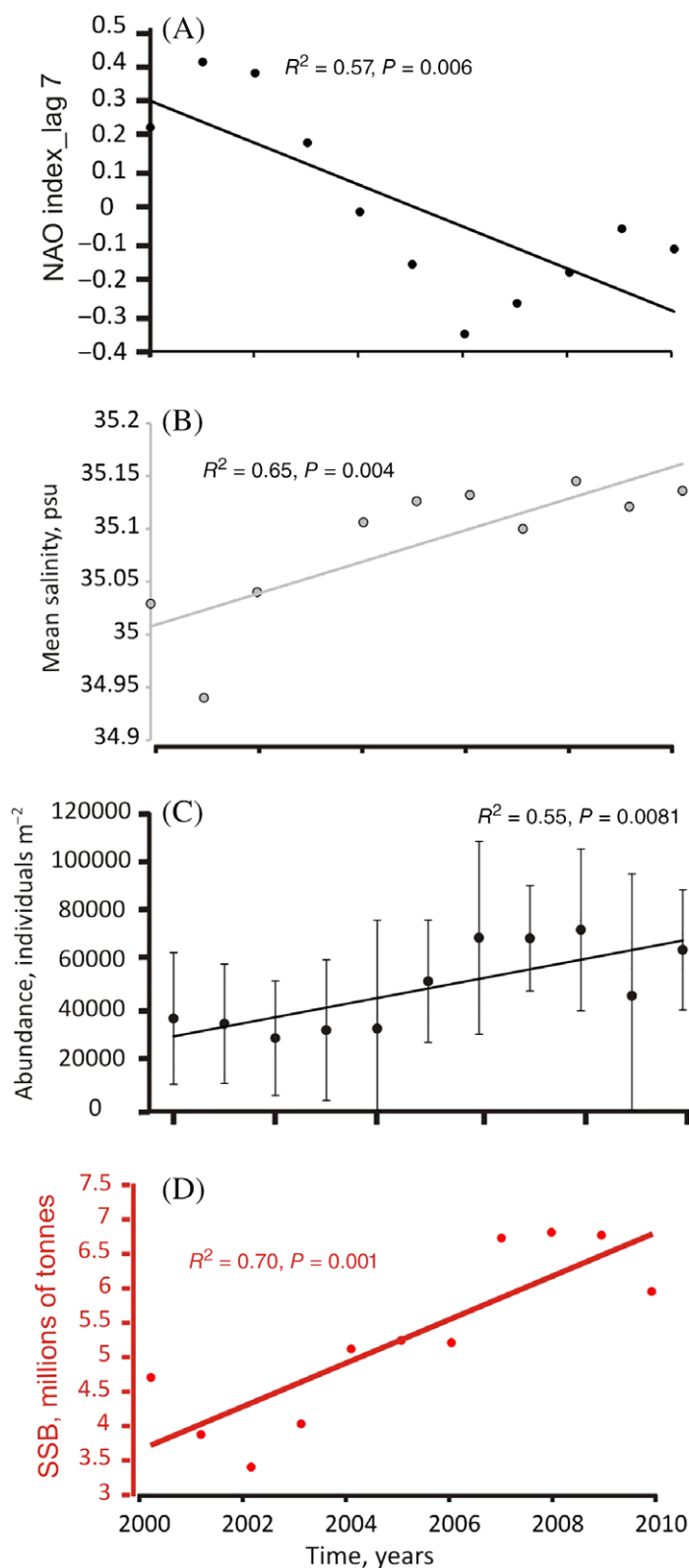
Fig. 8. Time series of the autumn mean of the lagged 7 yr NAO index (**A**), mean salinity at the AW layer (**B**), mean copepod abundances (**C**), and spring spawning biomass of herring (**D**). Continuous lines show linear fits.

Table 3. Results of pairwise Kendall's τ analyses between the 7 yr lagged winter NAO index, salinity of the AW layer, the thickness of that layer, copepod abundances, and herring spring SSB. Significant results were written in bold letters ($p < 0.05$)

	NAO index, lag 7	Salinity AW layer	Copepod abundance	Herring SSB
Salinity AW layer	**T = −0.60, p = 0.015**			
Copepod abundance	**T = −0.70, p = 0.002**	**T = 0.6, p = 0.015**		
Herring SSB	**T = −0.56, p = 0.015**	**T = 0.55, p = 0.025**	**T = 0.60, P = 0.008**	
AW layer thickness	**I = −0.53, p = 0.031**	**T = −0.76, p = 0.0019**	T = −0.44, p = 0.075	**T = −0.53, p = 0.031**

flows northeastward. These eddies affect the distribution of capelin larvae in the upper layers of the water column (Pedersen et al. 2005), and eddies have been shown to determine copepod distributions in many different upper layer systems (Mackas and Galbraith 2002; Fernandes 2008). However, mesoscale eddies can also drive circulation in deep oceanic layers down to 1000 m (Chelton et al. 2011; Zhang et al. 2014). Furthermore, the persistent eddies observed in the Lofoten Basin might intensify during winter months (Soiland and Rossby 2013). The observed patches of overwintering copepods between 700 and 900 m depth (Fig. 6) are thus likely due to passive concentration of copepods in mesoscale eddies.

Spatial patterns in copepod abundance varied greatly in their significance and shape depending on the year. This variability was persistent among abundance distributions (Fig. 4) and spatial correlograms (Fig. 5; Table 2). The fact that the clearest patterns were observed in the correlogram performed by pooling data from different years (Fig. 5) points to a significant effect of the number of stations sampled on the observed spatial assemblages. This effect is also supported by the correlograms done within the focus area (Table 2), where a significant fit was obtained only in 2008 when the highest number of stations were sampled (69 stations; Table 2).

Long-term trends—surface and water column environment

Temperature remained relatively constant in surface waters (Fig. 7), which is in agreement with analyses of satellite-retrieved SST trends for the Norwegian Sea during the first decade of the 21st century (Singh et al. 2013). These patterns match the general hydroclimatic forcing for those years, as between the mid 1990s and the mid 2000s, the dominant phase of the NAO was negative (Fig. 7E; Sarafanov et al. 2008), which indicates that westerly warm Atlantic winds and in turn the Atlantic Current were weaker (Frankignoul et al. 2009; Sarafanov 2009). Conversely, these observations do not match with the observed increase in thickness of the AW layer during the last years of the study period (Fig. 6). We observed a deepening of the limit between the Norwegian Sea Deep Water and the AW layer. Most likely, these thicker layers are not due to an increase in the AW inflow but due to an increase in the salinity and temperatures within the AW layer. Negative NAO forcing increases the contribution of warmer and saltier subtropical water masses to the formation of AW in the North

Atlantic (Holliday et al. 2008; Sarafanov et al. 2008; Sarafanov 2009). This process starts in the upper layers of the Labrador Sea (Fig. 1), thus its transmission to deeper waters and across the Atlantic Ocean takes several years (Sarafanov 2009). The eastward transmission of the opposite hydroclimatic signal driven by a positive NAO scenario, that is, the freshening of the AW layer, is known to have taken 7 yr in the 1970s (Dickson et al. 1988; Aksnes and Blindheim 1996). Furthermore, it took 6 yr for modeled copepods to spread over the scale of the North Atlantic (Speirs et al. 2006). Thus, our observed lag of 7 yr between NAO index and the salinity of the AW layer (Fig. 3) is consistent with these time scales. Because the increase in salinity is transmitted through the AW layers (Alekseev et al. 2001; Sarafanov 2009), density within the layer will increase.

Long-term trends—Copepods

The observed increase in overwintering copepod abundance in the Lofoten Basin from 2000 to 2010 (Fig. 8C) is in line with an increase in summer abundance from 2001 to 2009 further downstream in the Norwegian Atlantic Current and in the West Spitsbergen Current (Carstensen et al. 2012). It also matches with the increase in summer abundance of *C. finmarchicus* from 1995 to 2016 downstream in the Barents Sea (Aarflot et al. 2017). Both branches of the Norwegian Atlantic Current, the one continuing along the shelf edge toward the Fram Strait and the Arctic Ocean and the one turning into the Barents Sea (Fig. 1), advect large amounts of *C. finmarchicus* into the respective ecosystems (Edvardsen et al. 2003; Gluchowska et al. 2017; Basedow et al. 2018). For the Barents Sea, time scales of water mass advection and the proximity to overwintering habitats in the northern Norwegian Sea indicate that the temporal increase in overwintering stocks that was observed in our study might contribute directly to the increase in summer abundances in the Barents Sea (Aarflot et al. 2017). As discussed in Carstensen et al. (2012), time scales of advection might be too long for an overwintering stock in the Lofoten Basin to influence summer abundances in the West Spitsbergen Current directly. It is more likely that the observed increase in overwintering *Calanus* sp. abundances in the Lofoten Basin produces offspring generations that might overwinter in areas further north. Thus, the observed increases in overwintering abundance in the Lofoten Basin and summer abundances in the West

Spitsbergen likely respond to the same changes in environment, but are only indirectly linked. Advection from the southern Norwegian Sea most likely does not played a major role in the observed positive trends for *C. finmarchicus* in the Lofoten Basin, as from 2000 to 2010 a negative NAO scenario prevailed (Sarafanov et al. 2008). More probably, changes in the vertical structure of intermediate and deep water masses were affecting overwintering copepods.

AWs´ facilitation of vertical migration

The center of the vertical distribution of *Calanus* sp. was observed consistently just below the AW layer as in Gaardsted et al. (2011), and the WMD of copepods increased with an increase in the thickness of the AW layer over the years. Our own estimates of copepods´ WMD and those of copepods in the Northwestern Atlantic showed a significant variability in vertical distribution (Fig. 6; Krumhansl et al. 2018), but the fact that temporal trends in WMD mirrored those of the AW layer width clearly (Fig. 6) strongly suggests that density vertical structure is influencing the mean overwintering depth of *C. finmarchicus*. This means copepods have to migrate over larger vertical distances during onset and emergence to and from overwintering habitats. These vertical migration rates might be facilitated by saltier and thus denser background AW that were observed during the same period, and which correlated with copepod abundance. For a long time, the role of lipids in the vertical migration of copepods and other pelagic zooplankters was underestimated (Yayanos et al. 1978; Sargent and Falk-Petersen 1988; Lee et al. 2006). The copepods lipids consist primarily of wax esters (Sargent and Falk-Petersen 1988), and when the physical properties of these wax esters were investigated, it became clear that they were controlling the copepods buoyancy by changes in density driven by pressure and temperature changes across the water column (Childress and Nygaard 1974; Visser and Jonasdottir 1999). This relationship between depth of copepods and lipid content has been found for a wide range of species (Pond and Tarling 2011; Zarubin et al. 2014; Schmid et al. 2018).

For an effective buoyancy control of copepod vertical positioning, the background water density is as important as the lipid-mediated copepod density, because it is the difference between both that drives ascent and descent rates (Visser and Jonasdottir 1999). Changes in the internal lipid composition have been modeled to infer vertical movements and overwintering depths (Campbell and Dower 2003). However, little attention has been paid to the impact that changes in the density of the water masses can have on vertical positioning of copepods, regardless of the variability in copepod lipid content.

Here, we propose that an increase in salinity of the AW increased the relative density differences between copepods and water masses, and in turn favored vertical migration. The increase in salinity in AW was produced by a lagged large-scale forcing of the NAO, thus meaning overwintering depth of copepods was directly correlated to lagged climatic effects of the NAO. Paradoxically, dynamics within and below the AW, a layer that is not inhabited by *C. finmarchicus* for most of its life cycle, might be critical for copepod populations as they influence the performance of seasonal vertical migrations. In spring, passive upward migration is accelerated by a greater density contrast between copepods and saltier AW water, so that the copepods become positively buoyant faster while ascending (Fig. 9). The energy saved by these more efficient migrations might be of great importance for *C. finmarchicus* reproduction, as gonad formation depends entirely on those internal energy resources not consumed in winter (Tande and Hopkins 1981; Sargent and Falk-Petersen 1988; Jonasdottir 1999). This could explain the observed correlation among NAO, saltier AW water, and increased copepod abundances.

Dynamic links with higher trophic levels

The observed decreasing values of the NAO index, saltier AW, and increased abundance of overwintering copepods all correlated with increasing stocks of the Norwegain spring spawning herring. These correlations could be sequential: lagged effects of a negative NAO index increase salinity and density in the AW layers thus facilitating seasonal migration of *C. finmarchicus*, which in turn increases reproductive success and summer abundances, which then are fed on by herring and thus increase the biomass of the spawning stocks (Fig. 9). Although common temporal trends that are shared by most of the environmental and biological variables prevent the use of linear regressions, the nonparametric Kendall's τ estimates that we used show significant associations, which can be a cue of causal relationships. In addition, the NAO index, the main large-scale driver which could cause common independent trends in copepod and herring abundances has been considered in our analyses. It provided a causal explanation for increased AW layer depths and mean salinities and for the populations of copepods and herrings (Table 3). Higher abundances correlated to lower NAO index values have already been reported in *C. finmarchicus* and herrings in the North Sea, with a lag of 5 yr for the latter, but have not been successfully explained (Fromentin and Planque 1996; Gröger et al. 2010). In these previous studies, NAO-mediated effects on the density of intermediate/deep waters were not considered. In our study, significant statistical fits for the Lofoten Basin were found between the 7-yr lagged winter NAO index and the AW layer depth, between this depth and mean salinity, between mean salinity and copepod abundances, and between copepod abundances and herring stock biomass (Table 3), thus supporting a sequential, step-by-step mechanism.

Assuming a sequence of causal relationships, larger SSB of Norwegian spring spawning herring might be driven by bottom-up effects triggered by increased *C. finmarchicus* populations between 2000 and 2010. In contrast, Olsen et al. 2007 showed a top-down effect of Norwegian spring spawning herring on *C. finmarchicus*. These negative relationships between herring biomass and zooplankton abundances were found in the western Norwegian Sea, whereas further east in the Lofoten Basin,
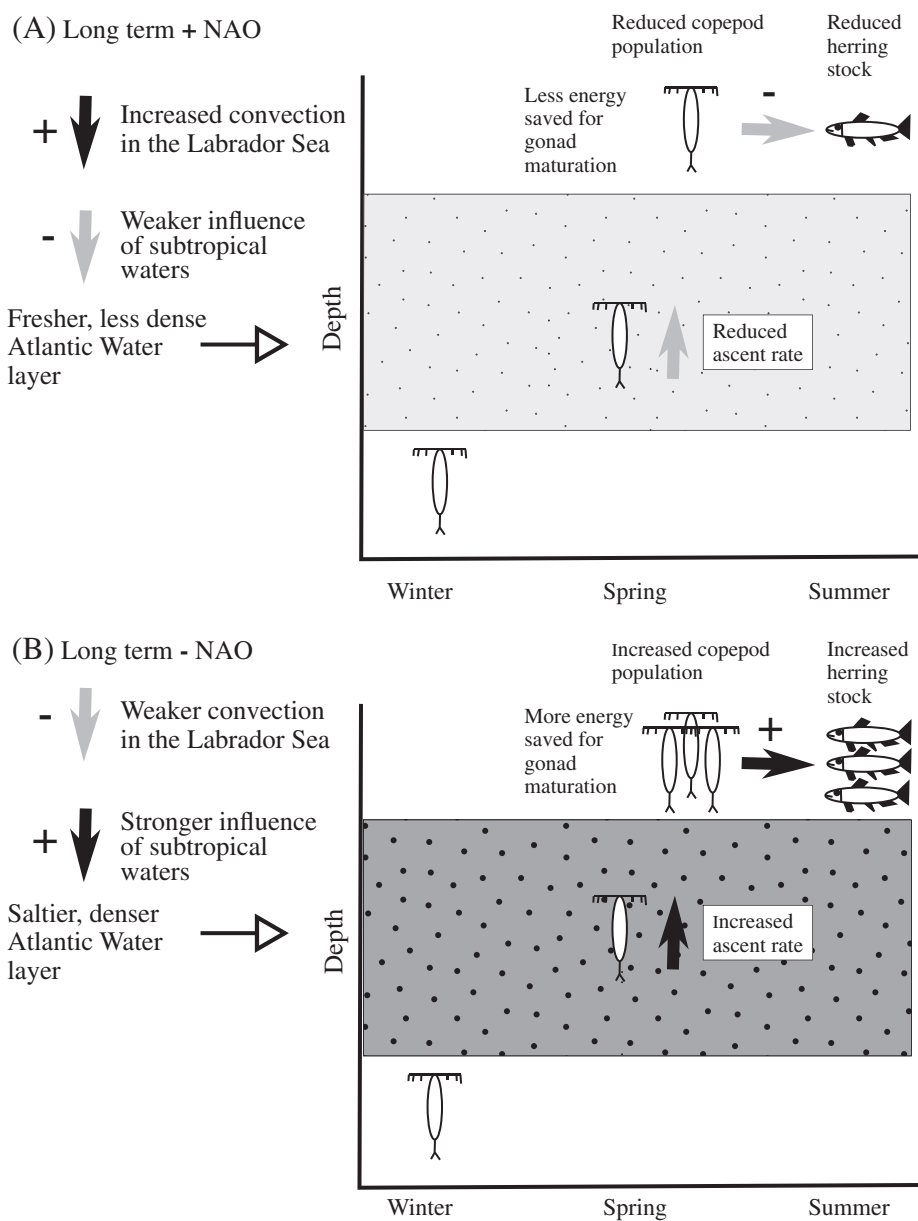
Fig. 9. Diagram representing seasonal migrations and reproduction of *C. finmarchicus* under positive (**A**) and negative (**B**) long-term NAO scenarios with respect to depth and time. The proposed hydroclimatic mechanism from NAO forcing to the spring spawning herring stock is shown for each scenario with arrows indicating negative and positive relationships. In panel **B**, a darker background with larger dots represents a saltier, denser AW layer.

this association was not observed (Olsen et al. 2007). The authors suggest that this lack of effect is caused by the lower overall zooplankton abundances to the east, but the timing of the herring seasonal migration across the Norwegian Sea might also explain the spatial variability in the predator–prey relationship. In the beginning of spring, herring usually moves from the spawning locations along the coast to the northwest (Huse 2016) and then feeds on recently ascended copepodite stage V and adult copepods (Generation 0, G0) that are ready to spawn. Predation on these sensitive G0 stages might cause a more negative effects and thus result in top-down control on copepod populations. In contrast, herrings move to the Lofoten Basin later in the season (June–July) and prey on the next generation G1 of CIV-CV stages just prior to their seasonal downward migration. Therefore, predation effects in these eastern regions might impact the populations to a lesser extent, thus enabling a bottom up effect.

Potential caveats

Each of the winter cruises was designed with different purposes, different methodologies, different levels of spatial resolution that were applied, and different total areas that were

surveyed (Fig. 1; Table 1). This introduces some degree of uncertainty when comparing overall AW layer thickness, copepod abundances, patch size, and WMD of copepods between the years. Nevertheless, it is unlikely that such uncertainty caused significant temporal trends in all these variables and we therefore consider our results to be robust against the potential uncertainties.

Conclusion

A well-studied climatic shift toward a negative NAO scenario, which started by the mid 1990s, changed the salinity in the Lofoten Basin, positively affecting seasonal vertical migrations of *C. finmarchicus*, and in turn its reproductive success and abundances in the region. Moreover, we found evidences that these effects may scale up to higher trophic levels, producing an increase in the SSB of Norwegian spring spawning herring. In essence, our study emphasizes the role of large-scale lagged hydrographic forcing in changing key oceanographic characteristics, even at great depths, affecting biologically and economically important components of the pelagic ecosystem.

References

Aarflot, J. M., H. R. Skjoldal, P. Dalpadado, and M. Skern-Mauritzen. 2017. Contribution of Calanus species to the mesozooplankton biomass in the Barents Sea. ICES J. Mar. Sci. **75**: 2342–2354. doi:10.1093/icesjms/fsx221

Aksnes, D. L., and J. Blindheim. 1996. Circulation patterns in the North Atlantic and possible impact on population dynamics of *Calanus finmarchicus*. Ophelia **44**: 7–28. doi:10.1080/00785326.1995.10429836

Alekseev, G. V., O. M. Johannessen, A. A. Korablev, V. V. Ivanov, and D. V. Kovalevsky. 2001. Interannual variability in water masses in the Greenland Sea and adjacent areas. Polar Res. **20**: 201–208. doi:10.1111/j.1751-8369.2001.tb00057.x

Bachiller, E., G. Skaret, L. Nøttestad, and A. Slotte. 2016. Feeding ecology of Northeast Atlantic mackerel, Norwegian spring-spawning herring and blue whiting in the Norwegian Sea. PLoS One **11**: e0149238. doi:10.1371/journal.pone.0149238

Barber, R. T., M. P. Sanderson, S. T. Lindley, F. Chai, J. Newton, C. C. Trees, D. G. Foley, and F. P. Chavez. 1996. Primary productivity and its regulation in the equatorial Pacific during and following the 1991-1992 El Niño. Deep-Sea Res. Part II **43**: 933–969.

Basedow, S. L., A. Sundfjord, W. J. von Appen, E. Halvorsen, S. Kwasniewski, and M. Reigstad. 2018. Seasonal variation in transport of zooplankton into the Arctic Basin through the Atlantic gateway, Fram Strait. Front. Mar. Sci. **5**: 194. doi:10.3389/fmars.2018.00194

Baumgartner, M. F., T. V. N. Cole, R. G. Campbell, G. J. Teegarden, and E. G. Durbin. 2003. Associations between North Atlantic right whales and their prey, *Calanus finmarchicus*, over diel and tidal time scales. Mar. Ecol. Prog. Ser. **264**: 155–166. doi:10.3354/meps264155

Baumgartner, M. F., and A. M. Tarrant. 2017. The physiology and ecology of diapause in marine copepods. Ann. Rev. Mar. Sci. **9**: 387–411. doi:10.1146/annurev-marine-010816-060505

Beaugrand, G. 2003. Long-term changes in copepod abundance and diversity in the north-East Atlantic in relation to fluctuations in the hydroclimatic environment. Fish. Oceanogr. **12**: 270–283.

Beaugrand, G., P. C. Reid, F. Ibañez, J. A. Lindley, and M. Edwards. 2002. Reorganisation of North Atlantic marine copepod biodiversity and climate. Science **296**: 1692–1694. doi:10.1126/science.1071329

Beaugrand, G., and R. R. Kirby. 2010. Climate, plankton and cod. Glob. Change Biol. **16**: 1268–1280. doi:10.1111/j.1365-2486.2009.02063.x

Buonaccorsi, J. P., J. S. Elkinton, S. R. Evans, and A. M. Liebhold. 2001. Measuring and testing for spatial synchrony. Ecology **82**: 1668–1679. doi:10.1890/0012-9658(2001)082[1668:MATFSS]2.0.CO;2

Campbell, R. W., and J. F. Dower. 2003. Role of lipids in the maintenance of neutral buoyancy by zooplankton. Mar. Ecol. Prog. Ser. **263**: 93–99. doi:10.3354/meps263093

Carstensen, J., A. Weydmann, A. Olszewska, and S. Kwasnieski. 2012. Effects of environmental conditions on the biomass of Calanus spp. in the Nordic seas. J. Plankton Res. **34**: 951–966. doi:10.1093/plankt/fbs059

Changnon, S. A. 1999. Impacts of 1997–98 El Niño–generated weather in the United States. Bull. Am. Meteorol. Soc. **80**: 1819–1827. doi:10.1175/1520-0477(1999)080<1819:IOENOG>2.0.CO;2

Chelton, D. B., M. G. Schlax, and R. M. Samelson. 2011. Global observations of nonlinear mesoscale eddies. Prog. Oceanogr. **91**: 167–216. doi:10.1016/j.pocean.2011.01.002

Childress, J. J., and M. Nygaard. 1974. Chemical composition and buoyancy of midwater crustaceans as a function of depth of occurrence off Southern California. Mar. Biol. **27**: 225–238. doi:10.1007/BF00391948

Conversi, A., S. Piontkovski, and S. Hameed. 2001. Seasonal and interannual dynamics of *Calanus finmarchicus* in the Gulf of Maine (northeastern US shelf) with reference to the North Atlantic oscillation. Deep-Sea Res. **48**: 519–530.

Currie, J. C., M. Lengaigne, J. Vialard, D. M. Kaplan, O. Aumont, S. W. A. Naqvi, and O. Maury. 2013. Indian Ocean dipole and El Niño/southern oscillation impacts on regional chlorophyll anomalies in the Indian Ocean. Biogeosciences **10**: 6677–6698. doi:10.5194/bg-10-6677-2013

Curry, R., B. Dickson, and I. Yashayaev. 2003. A change in the freshwater balance of the Atlantic Ocean over the past four decades. Nature **426**: 18–25.

Daase, M., J. O. Vik, E. Bagoien, N. C. Stenseth, and K. Elane. 2007. The influence of advection on Calanus near Svalbard: Statistical relations between salinity, temperature and

copepod abundance. J. Plankton Res. **29**: 903–911. doi: 10.1093/plankt/fbm068

Dickson, R. R., J. Meincke, S. A. Malmberg, and A. J. Lee. 1988. The "great salinity anomaly" in the northern North Atlantic 1968-1982. Prog. Oceanogr. **20**: 103–151. doi:10.1016/0079-6611(88)90049-3

Edvardsen, A., D. Slagstad, K. S. Tande, and P. Jaccard. 2003. Assesing zooplankton advection in the Barents Sea using underway measurements and modelling. Fish. Oceanogr. **12**: 61–74. doi:10.1046/j.1365-2419.2003.00219.x

Edvardsen, A., J. M. Pedersen, D. Slagstad, T. Semenova, and A. Timonin. 2006. Distribution of overwintering Calanus in the north Norwegian Sea. Ocean. Sci. **2**: 87–96. doi: 10.5194/os-2-87-2006

Falk-Petersen, S., P. Mayzaud, G. Kattner, and J. R. Sargent. 2009. Lipids and life strategy of Arctic Calanus. Mar. Biol. Res. **5**: 18–39. doi:10.1080/17451000802512267

Fernandes, V. 2008. The effect of semi-permanent eddies on the distribution of mesozooplankton in the central Bay of Bengal. J. Mar. Res. **66**: 465–488. doi:10.1357/002224008787157430

Frankignoul, C., J. Deshayes, and R. Curry. 2009. The role of salinity in the decadal variability of the North Atlantic meridional overturning circulation. Clim. Dyn. **33**: 777–793. doi:10.1007/s00382-008-0523-2

Fromentin, J. M., and B. Planque. 1996. Calanus and environment in the eastern North Atlantic. 11. Influence of the North Atlantic oscillation on *C. finmarchicus* and *C. helgolandicus*. Mar. Ecol. Prog. Ser. **134**: 111–118. doi:10.3354/meps134111

Gaardsted, F., K. S. Tande, and S. L. Basedow. 2010*a*. Measuring copepod abundance in deep-water winter habitats in the NE Norwegian Sea: Intercomparison of results from laser optical plankton counter and multinet. Fish. Oceanogr. **19**: 480–492.

Gaardsted, F., M. Zhou, V. Pavlov, A. Morozov, and K. S. Tande. 2010*b*. Mesoscale distribution and advection of overwintering *Calanus finmarchicus* off the shelf of northern Norway. Deep-Sea Res.Part I **57**: 1465–1473.

Gaardsted, F., K. S. Tande, and O. P. Pedersen. 2011. Vertical distribution of overwintering *Calanus finmarchicus* in the NE Norwegian Sea in relation to hydrography. J. Plankton Res. **33**: 1477–1486. doi:10.1093/plankt/fbr042

Gluchowska, M., P. Dalpadado, A. Beszczynska-Möller, A. Olszewska, R. B. Ingvaldsen, and S. Kwasniewski. 2017. Interannual zooplankton variability in the main pathways of the Atlantic water flow into the Arctic Ocean (Fram Strait and Barents Sea branches). ICES J. Mar. Sci. **74**: 1921–1936. doi:10.1093/icesjms/fsx033

Gröger, J. P., G. H. Kruse, and N. Rohlf. 2010. Slave to the rhythm: How large-scale climate cycles trigger herring (*Clupea harengus*) regeneration in the North Sea. ICES J. Mar. Sci. **67**: 454–465. doi:10.1093/icesjms/fsp259

Häfker, N. S., M. Teschke, K. S. Last, D. W. Pond, L. Hüppe, and B. Meyer. 2018. *Calanus finmarchicus* seasonal cycle and diapause in relation to gene expression, physiology,

and endogenous clocks. Limnol. Oceanogr. **63**: 2815–2838. doi:10.1002/lno.11011

Halvorsen, E., K. S. Tande, A. Edvardsen, D. Slagstad, and O. P. Pedersen. 2003. Habitat selection of overwintering *Calanus finmarchicus* in the NE Norwegian Sea and shelf waters off northern Norway in 2000–02. Fish. Oceanogr. **12**: 339–351.

Hamilton, L. C., J. S. Jonsson, H. Ogmundardottir, and I. M. Belkin. 2004. Sea changes ashore: The ocean and Iceland's herring capital. Arctic **57**: 325–335.

Heath, M. R., J. G. Fraser, A. Gislason, S. J. Hay, S. H. Jonasdottir, and K. Richardson. 2000. Winter distribution of *Calanus finmarchicus* in the Northeast Atlantic. ICES J. Mar. Sci. **57**: 1628–1635. doi:10.1006/jmsc.2000.0978

Herman, A. W., B. Beanlands, and E. F. Philliips. 2004. The next generation of optical planton counter. J. Plankton Res. **26**: 1135–1145.

Hirche, H. J. 1996. Diapause in the marine copepod, *Calanus finmarchicus*—a review. Ophelia **44**: 129–143. doi:10.1080/00785326.1995.10429843

Holliday, N. P., et al. 2008. Reversal of the1960s to 1990s freshening trend in the Northeast North Atlantic and Nordic seas. Geophys. Res. Lett. **35**: L03614. doi:10.1029/2007GL032675

Hunter, J. D. 2007. Matplotlib: A 2-D graphics environment. Comput. Sci. Eng. **9**: 90–95. doi:10.1109/MCSE.2007.55

Hurrell, J. W. 1995. Decadal trends in the North Atlantic oscillation: Regional temperatures and precipitation. Science **269**: 676–679. doi:10.1126/science.269.5224.676

Huse, G. 2016. A spatial approach to understanding herring population dynamics. Can. J. Fish. Aquat. Sci. **73**: 177–188. doi:10.1139/cjfas-2015-0095

Huse, G., and others. 2012. Effects of interactions between fish populations on ecosystem dynamics in the Norwegian Sea—results of the INFERNO project. **8**: 415–419.

Ingvarsdóttir, A., D. F. Houlihan, M. R. Heath, and S. J. Hay. 1999. Seasonal changes in respiration rates of copepodite stage V *Calanus finmarchicus* (Gunnerus). Fish. Oceanogr. **8**: 73–83. doi:10.1046/j.1365-2419.1999.00002.x

IPCC. 2014. Fifth assessment report. Cambridge Univ. Press. doi:10.2106/JBJS.ST.M.00041

Jakobsson, J. 1969. On herring migrations in relation to changes in sea temperature. Jokull **19**: 134–145 Marine Research Institute, Reykjavik.

Johnson, C. L., A. W. Leising, J. A. Runge, E. J. H. Head, P. Pepin, S. Plourde, and E. G. Durbin. 2007. Characteristics of *Calanus finmarchicus* dormancy patterns in the Northwest Atlantic. ICES J. Mar. Sci. **65**: 339–350.

Jonasdottir, S. H. 1999. Lipid content of *Calanus finmarchicus* during overwintering in the Faroe-Shetland Channel. Fish. Oceanogr. **8**: 61–72. doi:10.1046/j.1365-2419.1999.00003.x

Kimmel, D. G., and S. Hameed. 2008. Update on the relationship between the North Atlantic oscillation and *Calanus finmarchicus*. Mar. Ecol. Prog. Ser. **366**: 111–117. doi: 10.3354/meps07523

Krumhansl, K. A., E. J. H. Head, P. Pepin, S. Plourde, N. R. Record, J. A. Runge, and C. L. Johnson. 2018. Environmental drivers of vertical distribution in diapausing Calanus copepods in the Northwest Atlantic. Prog. Oceanogr. **162**: 202–222. doi:10.1016/j.pocean.2018.02.018

Lan, K. W., K. Evans, and M. A. Lee. 2013. Effects of climate variability on the distribution and fishing conditions of yellowfin tuna (*Thunnus albacares*) in the western Indian Ocean. Clim. Change **119**: 63–77. doi:10.1007/s10584-012-0637-8

Lee, R. F., W. Hagen, and G. Kattner. 2006. Lipid storage in marine zooplankton. Mar. Ecol. Prog. Ser. **307**: 273–306. doi:10.3354/meps307273

Lozier, M. S., and N. M. Stewart. 2008. On the temporally-varying northward penetration of Mediterranean OverflowWater and eastward penetration of Labrador Sea water. J. Phys. Oceanogr. **38**: 2097–2103. doi:10.1175/2008JPO3908.1

Mackas, D. L., and M. D. Galbraith. 2002. Zooplankton distribution and dynamics in a North Pacific Eddy of coastal origin: I. Transport and loss of continental margin species. J. Oceanogr. **58**: 725–738. doi:10.1023/A:1022802625242

Melle, W., and others. 2014. The North Atlantic Ocean as habitat for *Calanus finmarchicus*: Environmental factors and life history traits. Prog. Oceanogr. **129**: 244–284. doi:10.1016/j.pocean.2014.04.026

Mork, K. A., and O. Skagseth. 2010. A quantitative description of the Norwegian Atlantic current by combining altimetry and hydrography. Ocean. Sci. **6**: 901–911. doi:10.5194/os-6-901-2010

Olsen, E. M., W. Melle, S. Kaartvedt, J. C. Holst, and K. A. Mork. 2007. Spatially structured interactions between a migratory pelagic predator, the Norwegian spring-spawning herring *Clupea harengus* L., and its zooplankton prey. J. Fish Biol. **70**: 799–815. doi:10.1111/j.1095-8649.2007.01342.x

Orvik, K. A. 2004. The deepening of the Atlantic water in the Lofoten Basin of the Norwegian Sea, demonstrated by using an active reduced gravity model. Geophys. Res. Lett. **31**: L01306. doi:10.1029/2003GL018687

Pedersen, O. P., M. Zhou, K. S. Tande, and A. Edvardsen. 2005. Eddy formation on the coast of North Norway—evidenced by synoptic sampling. ICES J. Mar. Sci. **62**: 615e628.

Pershing, A. J., and others. 2015a. Evaluating trophic cascades as drivers of regime shifts in different ocean ecosystems. Philos. Trans. R. Soc. Lond. B Biol. Sci. **370**: 20130265.

Pershing, A. J., and others. 2015b. Slow adaptation in the face of rapid warming leads to collapse of the Gulf of Maine cod fishery. Science **350**: 809–812.

Planque, B., and S. D. Batten. 2000. *Calanus finmarchicus* in the North Atlantic: The year of Calanus in the context of interdecadal change. ICES J. Mar. Sci. **57**: 1528–1535. doi:10.1006/jmsc.2000.0970

Pond, D. W. 2012. The physical properties of lipids and their role in controlling the distribution of zooplankton in the oceans. J. Plankton Res. **34**: 443–453. doi:10.1093/plankt/fbs027

Pond, D. W., and G. A. Tarling. 2011. Phase transitions of wax esters adjust buoyancy in diapausing *Calanoides acutus*. Limnol. Oceanogr. **56**: 1310–1318. doi:10.4319/lo.2011.56.4.1310

Sale, F. P., and others. 2005. Critical science gaps impede use of no-take fishery reserves. Trends Ecol. Evol. **20**: 74–80.

Sarafanov, A. 2009. On the effect of the North Atlantic oscillation on temperature and salinity of the subpolar North Atlantic intermediate and deep waters. ICES J. Mar. Sci. **66**: 1448–1454. doi:10.1093/icesjms/fsp094

Sarafanov, A., A. Falina, A. Sokov, and A. Demidov. 2008. Intense warming and salinification of intermediate waters of southern origin in the eastern subpolar North Atlantic in the 1990s to mid-2000s. J. Geophys. Res. **113**: C12022. doi:10.1029/2008JC004975

Sargent, J. R., and S. Falk-Petersen. 1988. The lipid biochemistry of calanoid copepods. Hydrobiologia **167**: 101–114.

Sætre, R. 2007. The Norwegian coastal current—oceanography and climate. Tapir Academic Press.

Schmid, M. S., F. Maps, and L. Fortier. 2018. Lipid load triggers migration to diapause in Arctic Calanus copepods—insights from underwater imaging. J. Plankton Res. **40**: 311–325. doi:10.1093/plankt/fby012

Singh, R. K., M. Maheshwari, S. R. Oza, and R. Kumar. 2013. Long-term variability in Arctic Sea surface temperatures. Polar Sci. **7**: 233e240.

Slagstad, D., and K. S. Tande. 1996. The importance of seasonal vertical migration in across shelf transport of *Calanus finmarchicus*. Ophelia **44**: 189–205. doi:10.1080/00785326.1995.10429847

Soiland, H., and G. Huse. 2012. Using RAFOS floats to simulate overwinter transport of *Calanus finmarchicus* in the Norwegian Sea. Mar. Biol. Res. **8**: 502–507. doi:10.1080/17451000.2011.639780

Soiland, H., and T. Rossby. 2013. On the structure of the Lofoten Basin Eddy. J. Geophys. Res. **118**: 4201–4212. doi:10.1002/jgrc.20301

Speirs, D. C., W. S. C. Gurney, M. C. Heath, W. Horbelt, S. N. Wood, and B. A. de Cuevas. 2006. Ocean-scale modelling of the distribution, abundance, and seasonal dynamics of the copepod *Calanus finmarchicus*. Mar. Ecol. Prog. Ser. **313**: 173–192. doi:10.3354/meps313173

Tande, K. S., and C. C. E. Hopkins. 1981. Ecological investigations of the zooplankton community of Balsfjorden, northern Norway: The genital system in *Calanus finmarchicus* and the role of gonad development in overwintering. Mar. Biol. **63**: 159–164. doi:10.1007/BF00406824

Tiselius, P., A. Belgrano, L. Andersson, and O. Lindahl. 2016. Primary productivity in a coastal ecosystem: A trophic perspective on a long-term time series. J. Plankton Res. **38**: 1092–1102. doi:10.1093/plankt/fbv094

Tittensor, D. P., B. Deyoung, and C. L. Tang. 2003. Modelling the distribution, sustainability and diapause emergence timing of the copepod *Calanus finmarchicus* in the Labrador Sea. Fish. Oceanogr. **12**: 299–316.

Ullah, H., I. Nagelkerken, S. U. Goldenberg, and D. A. Fordham. 2018. Climate change could drive marine food web collapse through altered trophic flows and cyanobacterial proliferation. PLoS Biol. **16**: e2003446. doi:10.1371/journal.pbio.2003446

Urban, M. C., and others. 2016. Improving the forecast for biodiversity under climate change. Science **353**: aad8466. doi:10.1126/science.aad8466

Vang, B. 2015. Recovery and properties of oil from the copepod *Calanus finmarchicus*. Ph.D. dissertation. The Arctic Univ. of Norway.

Visbeck, M. H., J. W. Hurrell, L. Polvani, and H. M. Cullen. 2001. The North Atlantic oscillation: Past, present, and future. Proc. Natl. Acad. Sci. USA **98**: 12877.

Visser, A. W., and S. H. Jonasdottir. 1999. Lipids, buoyancy and the seasonal vertical migration of *Calanus finmarchicus*. Fish. Oceanogr. **8**: 100–106. doi:10.1046/j.1365-2419.1999.00001.x

Wood. 2006. Generalized additive models: An introduction with R. Chapman and Hall.

Yashayaev, I. 2007. Hydrographic changes in the Labrador Sea, 1960–2005. Prog. Oceanogr. **73**: 242–276. doi:10.1016/j.pocean.2007.04.015

Yayanos, A. A., A. A. Benson, and J. C. Nevenzal. 1978. The pressure–volume–temperature (PVT) properties of a lipid mixture from a marine copepod, *Calanus plumchrus*; implications for buoyancy and sound scattering. Deep-Sea Res. **25**: 257–268. doi:10.1016/0146-6291(78)90591-X

Zarubin, M., V. Farstey, A. Wold, S. Falk-Petersen, and A. Genin. 2014. Intraspecific differences in lipid content of calanoid copepods across fine-scale depth ranges within the photic layer. PLoS ONE **9**: e92935. doi:10.1371/journal.pone.0092935

Zhang, X., M. Roman, D. Kimmel, C. McGilliard, and W. Boicourt. 2006. Spatial variability in plankton biomass and hydrographic variables along an axial transect in Chesapeake Bay. J. Geophys. Res. **111**: C05S11.

Zhang, Z., W. Wang, and B. Qiu. 2014. Oceanic mass transport by mesoscale eddies. Science **345**: 322–324. doi:10.1126/science.1252418

Acknowledgments

Conflict of Interest

None declared